

# Beam-column behavior of concrete filled steel tubes

G. Campione† and N. Scibilia†‡

*Dipartimento di Ingegneria Strutturale e Geotecnica, Università di Palermo, Viale delle Scienze-I-90128, Italy*

*(Received January 10, 2002, Revised June 25, 2002, Accepted July 10, 2002)*

**Abstract.** In the present investigation the experimental and theoretical flexural and compressive behavior of short tubular steel columns filled with plain concrete and fiber-reinforced concrete (FRC) was examined. For a given length of the members, the effects of different geometry and dimensions of the transverse cross-section (square and circular) were investigated. Constituent materials were characterized through direct tensile tests on steel coupons and through compressive and split tension tests on concrete cylinders. Load-axial shortening and load-deflection curves were recorded for unfilled and composite members. Finally, simplified expressions for the calculus of the load-deflection curves based on the cross-section analysis were given and the ultimate load of short columns was predicted.

**Key words:** compressive tests; flexural tests; composite members; fiber-reinforced concrete; ultimate load; load-deflection curves.

---

## 1. Introduction

In the field of composite members interesting and very common examples are the concrete filled steel tubes (CFT) utilized e.g., for columns in high rise building. Several European and international codes (Eurocode 4 1994, LRFD 1994, CSA 1994) allow one to use composite columns in which the concrete is external to the steel profile (W-shapes partially or fully encased) or the concrete is inside the steel profile (circular, rectangular or square steel tubes filled with plain concrete).

For these structural members the main aspects to take into account (Cosenza and Pecce 2000, Shams and Saadeghvaziri 1997) are: - local and global buckling phenomena; - shape and mechanical characteristics of the steel transverse cross-section; - bond condition between concrete and steel; - out of straightness of steel profile and presence of residual stresses; - mechanical characteristics of concrete core in the hardened state (compressive and tensile strength, modulus of elasticity); - properties of concrete in the fresh state (shrinkage, creep etc). Further analytical and experimental researches (Schneider 1988, Uy 2000) have focused on the influence of some of the above mentioned aspects and also highlighted interest in the use of advanced filling materials, e.g., high strength concrete or fiber reinforced concrete (FRC).

In the case of using FRC as filling material, although the addition of fiber does not produce variations in the maximum bearing capacity of composite members (columns or beams), their use is more suitable than an increase in the thickness of the steel wall because: - it increases the ductility and the post-peak resources (Campione *et al.* 2001); - it significantly increases the fire resistance of composite members

---

† Assistant Professor

‡ Associate Professor

(Kodur and Lie 1995), in particular when high strength concrete (HSC) is utilized (HSC being particularly sensitive to fire as shown in Felicetti and Gambarova 1998).

The present research regards the experimental behavior of composite members made of steel profile filled with plain or fiber-reinforced concrete tested in uniaxial compression and in flexure. The aim of the research was to study the compressive and flexural behavior of composite members constituted by steel tubes filled with plain concrete or fiber-reinforced concrete.

In particular, in the present paper the variables investigated were the influence of the shape and dimensions of the transverse cross-section. Finally, a comparison is proposed between experimental and analytical values obtained through a simplified analytical model.

## 2. Experimental investigation

The experimental investigation was carried out by testing in axial compression and in flexure cold formed hollow steel tubes welded along their length and having circular and square cross-sections. Composite members tested in compression were stub-columns having length  $L_c = 400$  mm. Some of these had a circular cross-section with external diameter  $D = 127$  and  $113$  mm and corresponding thickness  $t = 3$  and  $4$  mm. Other members had a square cross-section with external side  $H = 100$  and  $120$  mm and thickness  $t = 3$  mm. In the cases of members with a circular cross-section the diameter-to-thickness ratios, defined as  $D/t$ , were  $42$  and  $28$  and the  $L_c/r$  ratios (with  $r = D/2$ ) were  $6.3$  and  $7.0$  respectively. In the cases of square sections the analogous ratios were  $H/t = 33$  and  $40$ , with  $L_c/r$  ( $r = H/2$ ) equal to  $8$  and  $6.7$ .

Steel members having the same transverse cross-section, but with length  $L = 800$  mm, were also tested in four-point bending tests. Some of these were unfilled, while others were filled with plain concrete or FRC. Hooked steel fibers having length  $L_f = 30$  mm and diameter  $\phi = 0.5$  mm were utilized in FRC in a volume percentage of  $1\%$  corresponding to  $80 \text{ kg/m}^3$ .

Referring to compressive tests on composite members, it has to be mentioned that the end portions of steel tubes were stiffened (see Fig. 1) by welding steel plates on them, thus avoiding premature and dangerous failure at the end portions of the specimens during the test.



Fig. 1 Arrangements of square specimens before testing

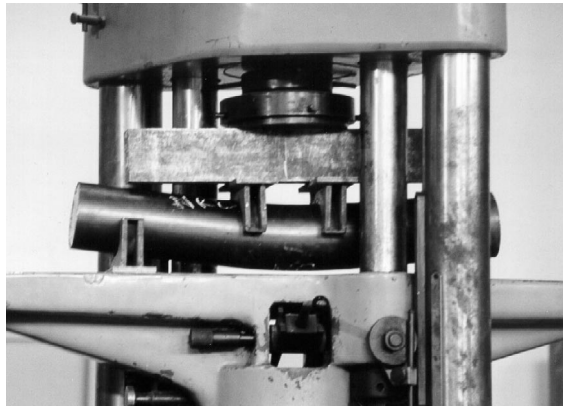


Fig. 2 Details of supports for circular steel tubes in flexure

To carry out flexure tests a four-point bending scheme was adopted and special end supports were arranged for cylindrical and prismatic specimens (see Fig. 2).

### 2.1. Mechanical characteristics of materials

The concrete utilized, having the characteristics and composition mentioned in other investigations by the authors (Campione *et al.* 2000), had compressive strength  $f_c$  measured on 100×200 mm cylinders at 28 days = 24 MPa, and splitting tensile strength  $f_t$  measured at 28 days on 100×200 mm cylinders = 2.84 MPa. The addition of fibers at 1% by volume did not change the compressive strength but it increased the tensile strength up to 3.29 MPa. The comparison of results relative to plain concrete and FRC showed that the addition of fibers produces: (a) modification of the post-peak response of the material; (b) no variations in maximum strength; (c) significant increases in compressive and tensile toughness and in maximum strain values (e.g., one order higher than for plain concrete was obtained by Campione *et al.* 1999).

To characterize the mechanical properties of the steel forming the tubes, steel coupons were extracted from the wall and tested in direct tension. The following average values were obtained: - yielding stress  $f_y = 338$  MPa, - ultimate stress  $f_u = 421$  MPa, - strain at failure  $\epsilon_u$  (measured on a gauge length of 50 mm) equal to 34%. Tests in compression on unfilled stub-columns have shown a slight reduction in yielding load with respect to the values determined through the tensile test, highlighting the role of initial stresses due to tube fabrication.

### 2.2. Test set-up

Compressive tests on short columns were carried out using a stiff universal testing machine having 3000 kN bearing capacity and equipped with spherical joints at the top allowing adjustments during the tests. Perfect adhesion between specimens and the steel end plates of the machine was created and specimens were directly loaded in both steel tubes and concrete core by means of a stiff steel plate. The results are inevitably affected by this particular loading procedure, as recently shown (Johansson and Kent 2001).

During the tests axial-shortening values were recorded by means of three linear voltage displacement



Fig. 3 Testing procedure of axially loaded columns

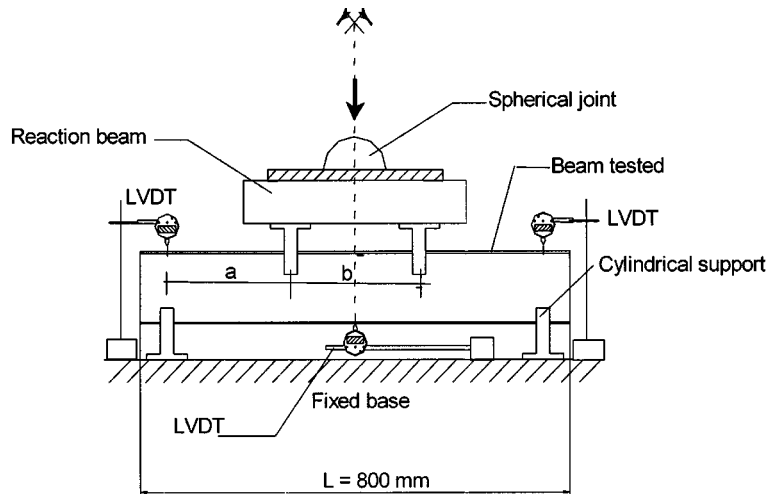


Fig. 4 Testing procedure of beam in flexure

transducer (LVDTs) placed on a gauge length equal to the entire length of the members (see Fig. 3). In this way the results are affected in the ascending branch of the response by local effects and the initial modulus of elasticity values are underestimated.

To perform flexural tests the test set-up shown in Fig. 4 was adopted. All the beams with 800 mm length were loaded in a four-point bending test, with a span of 690 mm between the supports. The ratio between the shear span  $a$  and the height of the beams was equal to 1.8 and 2.3 respectively for circular and square sections. Deformations were recorded by using LVDTs. One LVDT was placed in the lower part of the beams and recorded deflections; two other LVDTs were placed on the upper part of the beams in line with the supported sections. They were utilized to record settlements or local crushing of concrete or ovalization of the end steel cross-section of the beams. In this way it was possible to record the net deflection of the beams, purging the readings given by the middle LVDT of the settlements of the supports (these effects are significant in short members).

### 3. Experimental results

In this section experimental results of compressive and flexural tests on unfilled members and composite members are shown. Two tests for each type are presented.

Referring to compressive tests, in all the graphs in the ordinate there is the load  $P_v$  (recorded by the load cell) and in the abscissa the axial-shortening  $\delta_v$ .

Referring to flexural tests, in all the graphs in the ordinate there is the full load  $P$  (recorded by the load cell) and in the abscissa the net deflections  $\delta$ . For both the tests, because of the load-controlled test procedure, only the ascending branch of the response was recorded. Moreover, because of the short size and of the high thickness of the steel wall compared to the transverse dimensions, no strain gauges were utilized during the tests.

#### 3.1. Compressive behavior

Figs. 5(a) and (b) show load-shortening curves for columns of length 400 mm and having a circular cross-section of diameter 127 and 113 mm with wall thickness 3 and 4 mm, respectively. The same graphs presents results relating to unfilled columns and columns filled with plain concrete or FRC.

From the plots it emerges that the use of concrete inside steel tubes significantly increases the bearing capacity of unfilled columns and in the case of short columns complete yielding of materials occurs. Local buckling effects, visible to the eye, occur only after the peak load is reached. The use of FRC as filling material does not significantly increase the bearing capacity of composite members filled with plain concrete, but delays the local effects. Recent studies in the literature (Campione *et al.* 2000, Campione *et al.* 2001) referring to compressive displacement controlled tests on slender composite columns having circular cross-sections have shown that there are further advantages in using FRC as a filling material in the post-peak response (more ductility and less slope of the softening branch).

Fig. 6(a) and Fig. 6(b) show the analogous load-shortening curves for columns having a square section of wall thickness 3 mm and sides of 120 and 100 mm respectively. Similar results to those for composite members having a circular cross section were observed, but in the presence of FRC better performance, both in term of maximum strength and strain capacities, was observed. This is related to the higher effectiveness of fibers in confining and bridging cracks in square sections with respect to circular cross-sections.

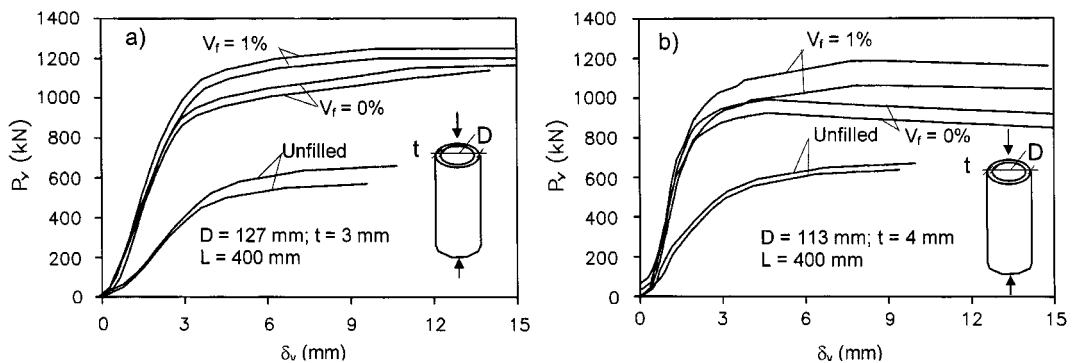


Fig. 5 Axial load-shortening curves for circular columns: a)  $D = 127$  mm; b)  $D = 113$  mm

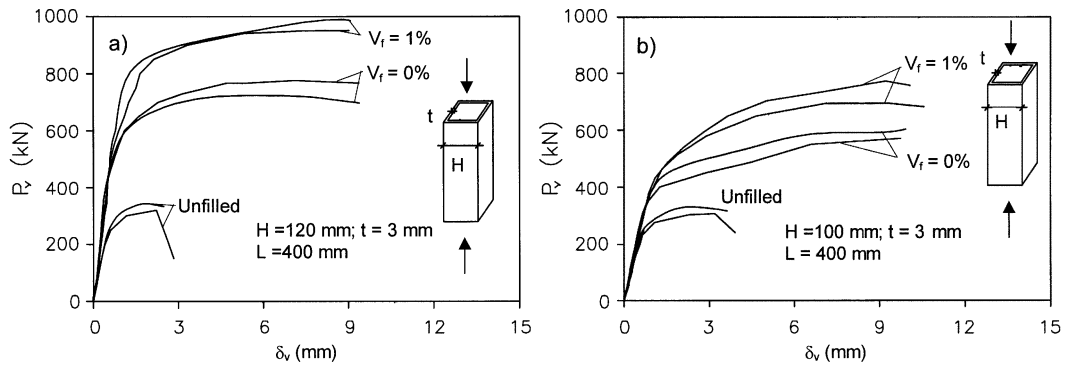


Fig. 6 Axial load-shortening curves for square columns: a)  $H = 120$  mm; b)  $H = 100$  mm



(a)



(b)

Fig. 7 Failure of columns in compression: a) circular columns; b) square columns

Fig. 7 shows the conditions of filled columns having circular and square specimens at the end of the test.

### 3.2. Flexural behavior

In this section load-deflection ( $P-\delta$ ) curves relating to flexural tests on unfilled and filled beams having circular and square cross-sections are shown.

Fig. 8(a) and Fig. 8(b) show results relating to circular cross-sections of 127 and 113 mm diameter for unfilled members and beams filled with plain concrete or FRC. For both the cases of 127×3 mm and 113×4 mm FRC filled tubes benefic effects due to the presence of fibers were observed.

All the responses were characterized by an initial elastic branch followed by the yielding of steel in tension governing the response up to failure. The yielding developed gradually due to the particular shape of the transverse cross-section (circular shape) and a very marked non-linear behavior was observed. For this reason it is difficult to define the yielding point accurately.

The contribution due to the presence of FRC was negligible and poorly affects the maximum bearing capacity of the composite beams, but higher deflections with no reduction in maximum

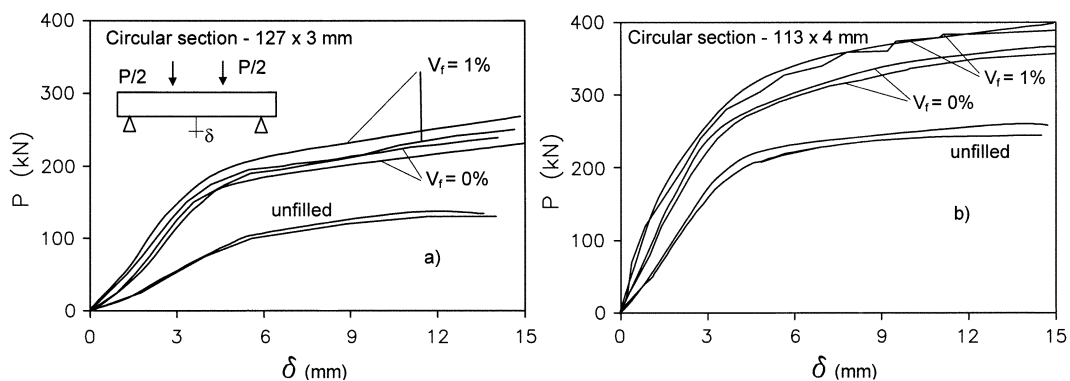


Fig. 8 Load-deflection diagrams for circular columns: a)  $D = 127$  mm; b)  $D = 113$  mm

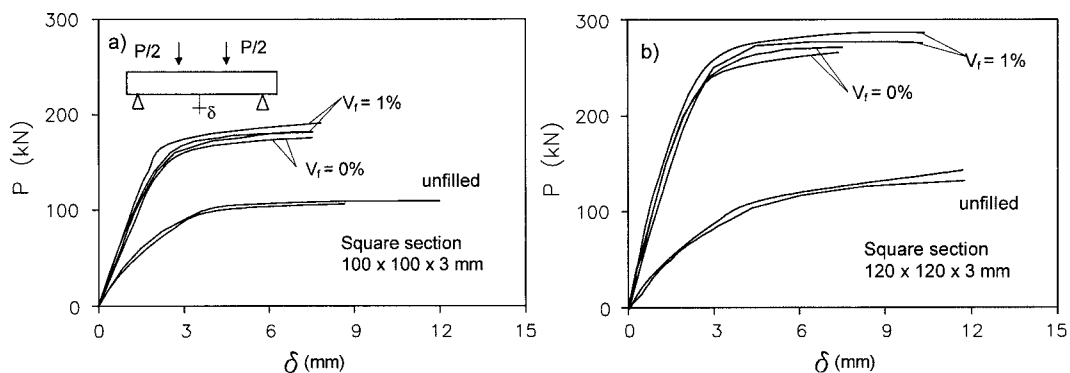


Fig. 9 Load-deflection diagrams for square columns: a)  $H = 120$  mm; b)  $H = 100$  mm

strength, were reached.

An analogous consideration can be made for the square cross-sections shown in Fig. 9(a) and Fig. 9 (b), respectively for members with sides of 100 and 120 mm. In this case the yielding point is clearly identifiable.

All results for flexural tests showed a good aptitude of composite beams to support bending moments. The presence of concrete prevented local buckling effects, and, despite the low shear span/height of the beam ratio, no reduction in the bearing capacity in pure bending was observed (as instead is generally expected in *R/C* members for shear-moment interaction).

#### 4. Analytical interpretation of experimental results

In the present section the bearing capacity of the short composite columns is calculated and analytical expressions for the moment-curvature relationship of composite beams are given.

Based on plane section analysis, in the hypothesis of perfect bond between concrete and steel profile up to failure, by integrating the curvature along the axis of the composite members the load-deflection curves are determined and compared with experimental results.

#### 4.1. Strength of compressed composite members

It is well known that if an axially compressed concrete cylinder is subjected to lateral compressive pressure, e.g., that induced by steel tubes filled with plain concrete, the maximum strength increases with respect to that of unconfined concrete. But the increase depends on the geometrical and mechanical characteristics of the steel tube and concrete core and also on the shape of the transverse cross-section of the member (Han *et al.* 2001). The confinement effect in the concrete core due to steel tube arises when the lateral expansion of concrete core exceeds the lateral expansion of the steel pipe. When high compressive stresses are achieved in concrete before the yielding of the steel tube in the longitudinal direction (the steel tube is in a biaxial stress state) the interaction between steel and concrete is effective. If the cross-sections of the steel pipe are slender no confinement effects are expected and the bearing capacity can at most reach the yielding strength due to the steel tubes and the compressive strength of the unconfined concrete core. If the ratio  $D/t$  (or  $H/t$ ) is increased, local buckling may occur before the yielding of steel and a reduction in the effective steel area has to be considered (Uy 2000).

If no local effects occur and increases in strength due to confinement effects in concrete core are neglected, it can be assumed that the bearing capacity  $P_{\max}$  is equal to:

$$P_{\max} = A_s \cdot f_y + A_c \cdot f_c \quad (1)$$

$A_c$  being the gross area of the transverse cross-section,  $A_s$  the area of the steel tube in the cross-section and  $f_c$  the compressive strength of the unconfined concrete. If the transverse cross-section is slender, e.g. if  $D/t > 90 \varepsilon^2$  for a circular section or  $H/t > 52 \varepsilon$  ( $\varepsilon = \sqrt{235/f_y}$ ) in accordance with Eurocode 4 (1994), the longitudinal stress has to be reduced.

Table 1 gives the geometrical and mechanical data of experimental tests recently proposed in the literature (Prion and Boheme 1993, Schenaider 1998, Uy 2000, Campione *et al.* 2000) and refers to axial compression tests on short composite members having circular or square transverse cross-sections. In all the tests presented, due to the reduced slenderness of the specimens (stub-columns), no reduction in the bearing capacity was observed due to buckling phenomena, as instead can occur for slender columns (Eurocode 4 1994). With reference to the axial compressive strength it was observed that the application of Eq. (1) gives results which are in agreement with the experimental data and a correlation factor of 0.91 was obtained.

Tests carried out by Prion and Boehme (1993) on cylindrical steel concrete filled columns have shown that after the peak load is reached shear failure may occur in the concrete core and an inclined failure plane forms with a reduction in the load-carrying capacity. As the concrete wedges slide past each other, the steel shell is fully activated as a circumferential tension band, resulting in a ductile failure mode at this secondary load level  $P_u$  lower than  $P_{\max}$ . Also, in the case of concrete members due to the lateral pressure confining compressed members at the maximum load an inclined failure plane forms in the concrete core and it is laterally restrained by the transverse steel (Issa and Tobaa 1994, Cusson and Paultre 1995).

Based on these considerations an analytical model is developed for predicting the load  $P_u$ , based on the rigid body equilibrium shown in Fig. 10.

When the failure plane in the concrete core forms, there act a force  $F_n$  and a friction force  $F_t$ ,  $F_t = \mu F_n$  where  $\mu$  is the friction coefficient. The horizontal force  $F_h$ , supposing the steel tubes to have yielded in the transverse direction, proves to be  $F_h = D t f_y / \tan \beta$ ,  $\beta$  being the angle that the failure plane forms

Table 1 Comparison of experimental data to predicted axial capacity

Ref. (n°)	Shape	$L_c$ (mm)	$H; D$ (mm)	$t$ (mm)	$\rho_s = 4t/D$	$f_c$ (MPa)	$f_y$ (MPa)	$P_{max}$ (kN) (exp)	$P_{max}$ Eq. (1)
(16)	circular	500	152	1.7	0.044	73	270	1548	1509
"	circular	500	152	1.7	0.044	73	270	1448	1509
"	circular	500	152	1.7	0.044	75	270	1545	1543
"	circular	900	152	1.7	0.044	75	270	1587	1543
"	circular	900	152	1.7	0.044	75	270	1458	1543
(18)	circular	602	140	3.0	0.070	28	285	881	761
"	circular	602	140	6.5	0.174	23	313	1825	1143
"	square	609	140	6.7	0.174	28	537	2715	2366
"	square	609	127	3.1	0.105	30	356	917	968
"	square	609	127	4.3	0.148	26	357	1095	1117
"	square	609	127	4.5	0.156	23	322	1113	1030
"	square	609	127	5.7	0.216	23	312	1207	1169
(19)	square	450	126	3.0	0.100	50	300	1114	1162
"	square	540	156	3.0	0.080	50	300	1708	1675
"	square	720	186	3.0	0.060	32	300	1555	1694
"	square	900	246	3.0	0.050	38	300	3095	3062
Present research	circular	400	127	3.0	0.094	24	338	1150	669
"	circular	400	113	4.0	0.141	24	338	975	566
"	square	400	100	3.0	0.120	24	338	590	605
"	square	400	120	3.0	0.100	24	338	720	642

(16) Prion and Boheme (1993); (18) Schenaider (1998); (19) Uy (2000).

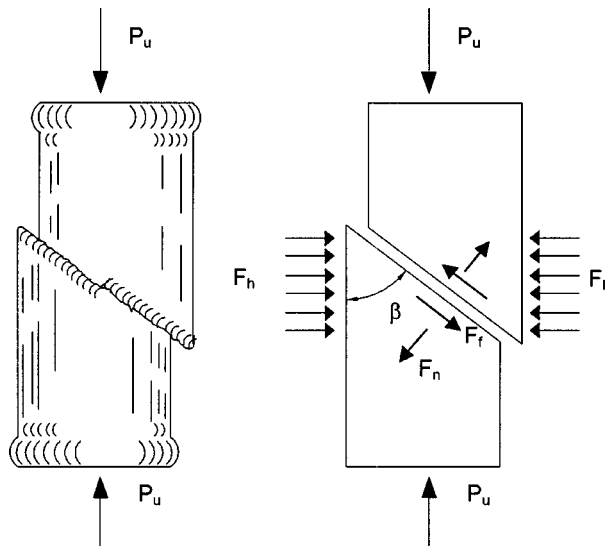


Fig. 10 Short column failure mode and model

with the vertical direction.

By considering the equilibrium of internal forces it is possible to obtain:

$$P_u = \frac{D}{\tan \beta} \cdot t \cdot f_y \cdot \left( \frac{\mu \cdot \cos \beta + \sin \beta}{\cos \beta - \mu \sin \beta} \right) \quad (2)$$

Cusson and Paultre (1995) have shown that, for high strength concrete (HSC) compressed members having a square section and confined with steel stirrups, the failure plane angle  $\beta$  depends on the effective confinement pressure. Similar effects were also observed by Prion and Boehme (1993) for composite members having circular cross-sections and filled with high strength concrete. If we assume  $\beta = 45^\circ$  and  $\mu = 0.5$  a value of  $P_u \approx 3 D \times f_y \times t$  is obtained.

#### 4.2. Moment-curvature and load-deflection curves for members in flexure

Referring to the cases examined in the previous section the moment-curvature relationships are determined. The first case examined (see Fig. 11) was that of unfilled steel tubes having square and circular cross-sections. For the steel constituting the tube only longitudinal stresses were considered and it was assumed that the behavior was linear-elastic up to the yielding point (at stress  $f_y$ ) and that afterwards a linear strain-hardening phase followed with a reduced slope (the initial stiffness was  $f_y / \varepsilon_y$  and the reduced stiffness was  $(f_u - f_y) / (\varepsilon_u - \varepsilon_y)$ ). This phase was extinguished at the ultimate strain  $\varepsilon_u$  (determined by uniaxial tests on coupons). Consequently, in the case of a circular cross-section the moment-curvature relationship was linear up to the yielding moment  $M_y = f_y \times W$  ( $W$  being the elastic modulus of the cross-section) and then expressed through the following relationship ( $M-\theta_0$ ):

$$M = \frac{2f_y r^2 t}{\cos \theta_0} \left( \frac{\pi}{2} - \theta_0 - \sin \cdot \theta_0 \cos \cdot \theta_0 \right) + 2 \frac{f_u - f_y}{(1 - \cos \cdot \theta_0^*)} r^2 t (\theta_0 - \sin \cdot \theta_0 \cos \cdot \theta_0) \quad (3)$$

with  $\theta_0$  being the angle (see Fig. 11) corresponding to the end of the elastic range in the cross-section linked to the curvature  $\chi$  by the following expression  $\chi = \frac{\varepsilon_y}{r \cdot \cos \theta_0}$  and  $\theta_0^* = \arccos \cdot \left( \frac{\varepsilon_y}{\varepsilon_u} \right)$ .

Analogously, in the case of a square section after the yielding point the moment-curvature relationship was:

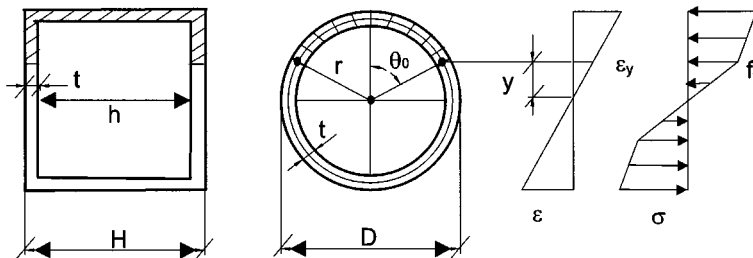


Fig. 11 Analytical model for section analysis of steel profile

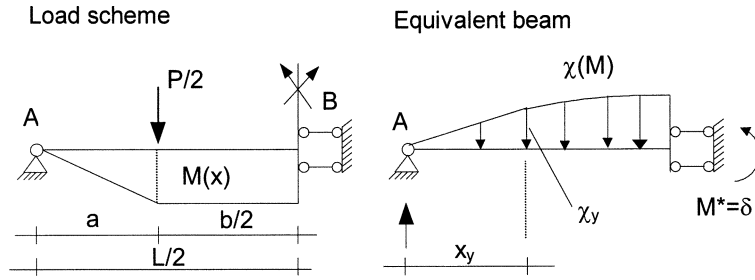


Fig. 12 Analytical model for load-deflection prediction

$$M = \frac{f_4}{4}(H^3 - h^3) - \frac{f_y}{3}\left(\frac{\epsilon_y}{\chi}\right)^2(H-h) + \frac{f_u - f_y}{12H^*}(H^4 - h^4) + \frac{f_u - f_y}{4H^*}\left(\frac{\epsilon_y}{\chi}\right)(H^3 - h^3) + \frac{f_u - f_y}{3H^*}\left(\frac{\epsilon_y}{\chi}\right)^3(H-h) \quad (4)$$

where

$$\chi = \frac{\epsilon_y}{y} \text{ and } H^* = H/2 \cdot \left(1 - \frac{\epsilon_y}{\epsilon_u}\right) \quad (5)$$

Similar expressions can also be utilized when local effects are expected, but as suggested in the literature (Sohal and Chen 1987, Sohal and Chen 1988) the ultimate strain values have to be reduced, depending on the steel grade and on the slenderness of the transverse cross-section.

For the determination of load-deflection curves based on the given moment-curvature relationships and referring to the equivalent beam of Fig. 12 and to the equilibrium conditions it is possible to obtain:

$$\delta\left(\frac{L}{2}\right) = \frac{P \cdot a}{2 \cdot E \cdot J} \left[ \frac{a^2}{3} + \frac{b^2}{8} + \frac{ab}{2} \right] \quad M < M_y \quad (6)$$

$$\delta\left(\frac{L}{2}\right) = \frac{\chi_y}{6}(a^2 + a \cdot x_y) + \frac{\chi_{\max}}{24} \cdot (8a^2 + 3b^2 - 4x_y^2 + 12ab - 4a \cdot x_y) \quad M > M_y \quad (7)$$

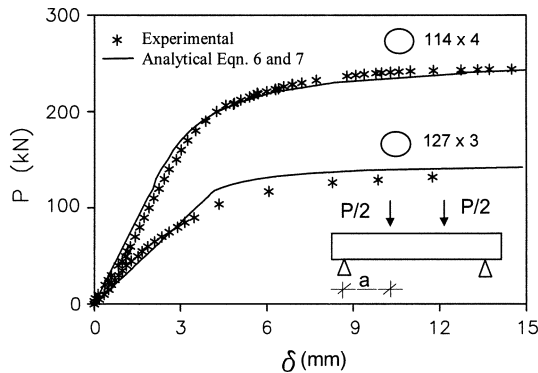


Fig. 13 Experimental and analytical comparisons of flexure tests for circular unfilled members

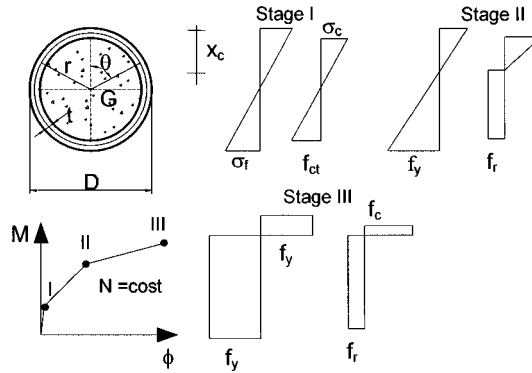


Fig. 14 Analytical model for section analysis of composite members

where  $\delta\left(\frac{L}{2}\right)$  is the deflection of the beams,  $P$  the external load,  $a$  and  $b$  the geometrical characteristics of the beams,  $J$  the moment of inertia of the beam,  $E$  the modulus of elasticity of the steel,  $\chi_y$  and  $\chi_{\max}$  the curvature at yielding and at the ultimate state and finally  $x_y$ ,  $x_{\max}$  the corresponding abscissas.

In Fig. 13 there are plotted the experimental and analytical load-deflection curves for unfilled beams, showing the good agreement obtained.

In the case of composite members it is possible to obtain numerically the moment-curvature relationships by using a computer program based on non-linear analysis. In a simplified way these relationships are obtained here (see Fig. 14) referring to the plane section hypothesis of cross-section subjected to axial forces and bending moment in three fundamental states: (a) I - first cracking of concrete in tension, (b) II - yielding of steel in tension and (c) III - ultimate condition. To reach these three states only increases in bending moment and constant axial force were considered.

It was supposed that the steel forming the pipe behaved in an elastic-plastic manner (strain hardening is here neglected for simplicity) and that the concrete core behaved elastically up to the first cracking. Later on, in the case of FRC a constant residual strength in tension  $f_r$  was considered and it was assumed, as suggested in Campione *et al.* (1999), that it varied with the amount and geometrical characteristics of the fibers. For concrete in compression linear behavior was assumed up to the yielding of the steel. At the ultimate state a uniform stress-block was assumed for both concrete and steel. No reduction in the maximum strength  $f_c$  of the unconfined concrete was made in order to take into account the confining action exerted by the steel tubes external to the concrete core. The model performs very well if perfect bond exists up to the ultimate state, but, as observed in Boedle *et al.* (1989), if local slippage occurs, a reduction in ultimate moment has to be considered.

In the case of a circular cross-section and referring to the ultimate state (state III of Fig. 14) the following simplified expressions of the axial force  $N$  and ultimate moment  $M$  were obtained in Campione *et al.* 2001:

$$N = \frac{1}{2} \cdot r^2 \cdot (\theta - \sin\theta) \cdot f_c + t \cdot \left(r + \frac{t}{2}\right) \cdot \theta \cdot f_y - t \cdot \left(r + \frac{t}{2}\right) \cdot (2\pi - \theta) \cdot f_y + -\frac{1}{2} \cdot r^2 \cdot (2\pi - \theta + \sin\theta) \cdot f_r \quad (8)$$

$$M = \frac{1}{2} \cdot r^2 \cdot (\theta - \sin\theta) \cdot f_c \cdot x_{c1} + t \cdot \left(r + \frac{t}{2}\right) \cdot \theta \cdot f_y \cdot x_{s1} + t \cdot \left(r + \frac{t}{2}\right) \cdot (2\pi - \theta) \cdot f_y \cdot x_{s2} + \frac{1}{2} \cdot r^2 \cdot (2\pi - \theta + \sin\theta) \cdot f_r \cdot x_{c2} \quad (9)$$

$x_{c1}$  and  $x_{s1}$  being the distance of the centers of the compressed zones from the center of the section  $G$ , having the following expressions:

$$x_{c1} = \frac{4}{3} \cdot r \cdot \frac{\sin^3\left(\frac{\theta}{2}\right)}{(\theta - \sin\theta)} \quad x_{s1} = \frac{2}{\theta} \left(r + \frac{t}{2}\right) \cdot \sin\left(\frac{\theta}{2}\right) \quad (10)$$

$x_{c2}$  and  $x_{s2}$  being the analogous quantities for the tension zone of steel obtained through Eq. (10) by using  $2\pi - \theta$  instead of  $\theta$ .

Table 2 and Table 3 give in an extended form the expressions of equilibrium equations in the elastic,

Table 2 Axial forces and bending moments in state I, II, II for square concrete filled members

Equations
<p>I Cracking</p> $N = \frac{nf_{ct}}{2} \cdot \frac{2x_c - t}{H - x_c - t} Ht + nf_{ct} \frac{x_c - t}{H - x_c - t} t(x_c - t) - nf_{ct} t(H - x_c - t) - nf_{ct} \left[1 + \frac{H - x_c}{H - x_c - t}\right] tH$ $+ \frac{1}{2} f_{ct} \frac{x_c - t}{H - x_c - t} h(x_c - t) - f_{ct} \frac{h}{2} (H - x_c - t)$ $M = \frac{n \cdot f_{ct}}{2} \cdot \frac{2x_c - t}{H - x_c - t} Ht \left(x_c + \frac{t}{2}\right) + n \cdot f_{ct} \frac{(x_c - t)^3}{H - x_c - t} t - \frac{2}{3} n \cdot f_{ct} t(H - x_c - t)^2 + nf_{ct} \left[1 + \frac{H - x_c}{H - x_c - t}\right] tH$ $\left(H - x_c - \frac{t}{2}\right) + \frac{1}{3} f_{ct} \frac{x_c - t}{H - x_c - t} h(x_c - t)^2 + \frac{f_{ct}}{3} h(H - x_c - t)^2$ $n = E/E_c; \quad \chi_f = \frac{f_{ct}}{E_{ct}(H - x_c - t)}$
<p>II Yielding</p> $N = \frac{f_y}{2} \left(2 - \frac{t}{x_c}\right) Ht + f_y t \frac{(x_c - t)^2}{x_c} - f_y t \frac{(H - x_c - t)^2}{x_c} - \frac{f_y (2H - 2x_c - t)}{2} tH + \frac{1}{2n} \left(1 - \frac{t}{x_c}\right) (x_c - t) h - f_r (H - x_c - t) h$ $M = \frac{f_y}{2} \left(2 - \frac{t}{x_c}\right) Ht \left(x_c - \frac{t}{2}\right) + \frac{2}{3} f_y t \frac{(x_c - t)^3}{x_c} - \frac{2}{3} f_y t \frac{(H - x_c - t)^3}{x_c} + \frac{f_y (2H - 2x_c - t)}{2} tH \left(H - x_c - \frac{t}{2}\right) +$ $+ \frac{1}{3n} \left(1 - \frac{t}{x_c}\right) (x_c - t)^2 h + \frac{f_r}{2} (H - x_c - t)^2 h$ $\chi_y = \frac{\epsilon_y}{x_c}$
<p>III Ultimate</p> $N = f_y 2t(x_c - t) + f_y 2t(x_c + t) + f_c h(x_c - t) - f_r h(H - x_c - t)$ $M = f_y Ht \left(x_c - \frac{t}{2}\right) + f_y t(x_c - t)^2 - f_y t(H - x_c - t)^2 + f_y Ht \left(H - x_c - \frac{t}{2}\right) + f_c \frac{h}{2} (x_c - t)^2 - f_r \frac{h}{2} (H - x_c - t)^2$

Table 3 Axial forces and bending moments in state I, II, II for circular CFT

Equations
<p><b>I - Cracking</b></p> $N = \frac{f_{ct}}{(D-x_c)} \left\{ r^2 \left[ \left( \frac{D}{2} - x_c \right) \left( \arccos \left[ \frac{1}{r} \left( \frac{D}{2} - x_c \right) \right] - \sqrt{1 - \left[ \frac{1}{r} \left( \frac{D}{2} - x_c \right) \right]^2} \frac{1}{r} \left( \frac{D}{2} - x_c \right) \right) - \frac{2}{3} r \left( \sqrt{1 - \left[ \frac{1}{r} \left( \frac{D}{2} - x_c \right) \right]^2} \right)^3 \right] + \right.$ $+ n' r^2 \left[ \left( \frac{D}{2} - x_c \right) \left( \pi - \arccos \left[ \frac{1}{r} \left( \frac{D}{2} - x_c \right) \right] + \sqrt{1 - \left[ \frac{1}{r} \left( \frac{D}{2} - x_c \right) \right]^2} \frac{1}{r} \left( \frac{D}{2} - x_c \right) \right) + \frac{2}{3} r \left( \sqrt{1 - \left[ \frac{1}{r} \left( \frac{D}{2} - x_c \right) \right]^2} \right)^3 \right] + \right.$ $\left. + n \left( r + \frac{t}{2} \right) t \left( \frac{D}{2} - x_c \right) \pi \right\}$ $M = \frac{f_{ct}}{(D-x_c)} \left\{ -r^3 \left[ \frac{(D-2x_c)}{3} \left( \sqrt{1 - \left[ \frac{1}{r} \left( \frac{D}{2} - x_c \right) \right]^2} \right)^3 + \right.$ $- r \left( -\frac{1}{2} \sqrt{1 - \left[ \frac{1}{r} \left( \frac{D}{2} - x_c \right) \right]^2} \right) \left( \frac{1}{r} \left( \frac{D}{2} - x_c \right) \right)^3 + \frac{1}{4} \sqrt{1 - \left[ \frac{1}{r} \left( \frac{D}{2} - x_c \right) \right]^2} \frac{1}{r} \left( \frac{D}{2} - x_c \right) + \frac{1}{4} \arccos \left[ \frac{1}{r} \left( \frac{D}{2} - x_c \right) \right] \right) + \right.$ $- n' r^3 \left[ -\frac{(D-2x_c)}{3} \left( \sqrt{1 - \left[ \frac{1}{r} \left( \frac{D}{2} - x_c \right) \right]^2} \right)^3 + \right.$ $\left. r \left( \frac{1}{2} \sqrt{1 - \left[ \frac{1}{r} \left( \frac{D}{2} - x_c \right) \right]^2} \right) \left( \frac{1}{r} \left( \frac{D}{2} - x_c \right) \right)^3 - \frac{1}{4} \sqrt{1 - \left[ \frac{1}{r} \left( \frac{D}{2} - x_c \right) \right]^2} \frac{1}{r} \left( \frac{D}{2} - x_c \right) - \frac{1}{4} \arccos \left[ \frac{1}{r} \left( \frac{D}{2} - x_c \right) \right] \right) + \right. \left. + n \left( r + \frac{t}{2} \right)^3 t \pi \right\}$ <p><math>n = E_c/E</math>; <math>n' = E_{ct}/E_c</math>; <math>x_c = R(1 - \cos \theta)</math>; <math>\varepsilon_y = f_y/E</math></p>
<p><b>II - Yielding</b></p> $N = \frac{E_c \varepsilon_y^2}{(D-x_c)} \left\{ \left( \frac{D}{2} - x_c \right) \left( \arccos \left[ \frac{1}{r} \left( \frac{D}{2} - x_c \right) \right] - \sqrt{1 - \left[ \frac{1}{r} \left( \frac{D}{2} - x_c \right) \right]^2} \frac{1}{r} \left( \frac{D}{2} - x_c \right) \right) - \frac{2}{3} r \left( \sqrt{1 - \left[ \frac{1}{r} \left( \frac{D}{2} - x_c \right) \right]^2} \right)^3 \right\} +$ $+ f_{ct} r^2 \left[ \sqrt{1 - \left[ \frac{1}{r} \left( \frac{D}{2} - x_c \right) \right]^2} \frac{1}{r} \left( \frac{D}{2} - x_c \right) - \arccos \left[ \frac{1}{r} \left( \frac{D}{2} - x_c \right) \right] + \pi \right] + \frac{E \varepsilon_y \pi}{(D-x_c)} \left( r + \frac{t}{2} \right) t [D - 2x_c]$ $M = \frac{E_c \varepsilon_y r^2}{(D-x_c)} \left\{ \frac{1}{3} \left( \sqrt{1 - \left[ \frac{1}{r} \left( \frac{D}{2} - x_c \right) \right]^2} \right)^3 (2x_c - D) + \frac{1}{4} \sqrt{1 - \left[ \frac{1}{r} \left( \frac{D}{2} - x_c \right) \right]^2} \left( \frac{D}{2} - x_c \right) + \right.$ $\left. \left[ -\frac{r}{2} \sqrt{1 - \left[ \frac{1}{r} \left( \frac{D}{2} - x_c \right) \right]^2} \left[ \frac{1}{r} \left( \frac{D}{2} - x_c \right) \right]^3 + \frac{r}{4} \arccos \left[ \frac{1}{r} \left( \frac{D}{2} - x_c \right) \right] \right] \right\}$ $+ \frac{2}{3} f_{ct} r^3 \left( \sqrt{1 - \left[ \frac{1}{r} \left( \frac{D}{2} - x_c \right) \right]^2} \right)^3 + \frac{E \varepsilon_y \pi}{(D-x_c)} t \left( r + \frac{t}{2} \right)^3$
<p><b>III Ultimate</b> See Eq. (8, 9, 10)</p>

yielding and ultimate states for square and circular cross-sections. In Table 4 are given analytical expressions for load-deflection curves for CFT in flexure at the different states examined.

Table 4 Load-deflection relationships for concrete filled members

Equations
<p>For <math>\chi_{\max} &lt; \chi_f</math></p> $\delta\left(\frac{L}{2}\right) = \chi_{\max} \left[ \frac{a^2}{3} + \frac{b^2}{8} + \frac{ab}{2} \right]$ <p>Being <math>\chi_f = \frac{\epsilon_{ct}}{H - x_c - t}</math></p>
<p>For <math>\chi_f &lt; \chi_{\max} &lt; \chi_y</math></p> $\delta\left(\frac{L}{2}\right) = \chi_f' \cdot \left[ \frac{a^2}{3} - \frac{a(a-x_f)}{2} + \frac{(a-x_f)^2}{6} \right] + \chi_{\max} \cdot \left[ \frac{ab}{2} + \frac{a(a-x_f)}{2} + \frac{b^2}{8} - \frac{(a-x_f)^2}{6} \right]$ <p>being <math>\chi_f'</math> with <math>\frac{\chi_f}{\chi_f}</math> <math>x_f</math> the abscissa at which first cracking occurs</p>
<p>For <math>\chi_y &lt; \chi_{\max} &lt; \chi_u</math></p> $\delta\left(\frac{L}{2}\right) = \chi_f' \cdot \left[ \frac{a^2}{3} - \frac{a(a-x_f)}{2} + \frac{(a-x_f)^2}{6} \right] + \chi_y' \cdot \left[ \frac{a(x_y-x_f)}{6} + \frac{(x_y^2-x_f^2)}{6} \right] + \chi_{\max} \cdot \left[ \frac{ab}{2} + \frac{a(a-x_f)}{2} + \frac{b^2}{8} - \frac{(a-x_f)^2}{6} \right]$ <p>being <math>\chi_y' = \frac{\chi_f}{x_f} \cdot a</math>, <math>\chi_y = \chi_f + \frac{(\chi_y - \chi_f)}{(x_y - x_f)} \cdot (a - \chi_f)</math>, <math>\chi_y = \frac{f_y}{E \cdot x_c}</math></p>

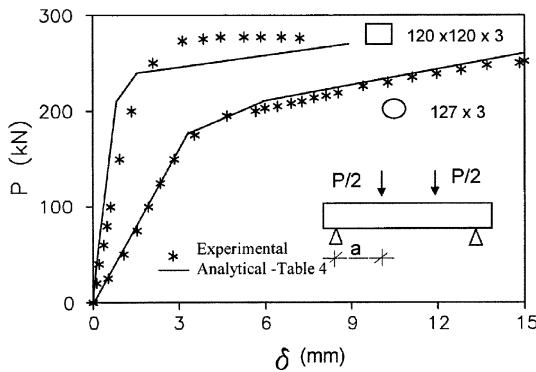


Fig. 15 Experimental and analytical comparisons of flexure tests for concrete filled members

Fig. 15 shows, referring, for brevity, only to the cases of square tubes 120×3 mm and circular filled tubes 127×3 mm, the acceptable agreement between analytical and experimental results referring to the composite members tested in the present investigation.

## 5. Conclusions

Based on experimental tests carried out in compression and in flexure on composite members made of steel tubes filled with plain concrete or fiber-reinforced concrete the following conclusions can be drawn:

- 1) in the case of short columns in compression the presence of concrete (plain or FCR) inside steel tubes increases the bearing capacity with respect to unfilled columns and this effect is more evident in the case of a square section;
- 2) in flexural tests the behavior of composite members is strongly influenced by steel characteristics and the presence of FRC does not alter the maximum bearing capacity of beams with respect to beams filled with plain concrete;
- 3) the presence of FRC inside steel tubes determines higher values of deformation at the maximum load. Finally, regarding the analytical contribution it can be observed that:
- 4) the simplified expression given for the calculus of the maximum bearing capacity (also given in the most common codes), based on the superposition of contributions by steel yielding and concrete crushing, furnishes valuable and conservative values of the maximum load for stub-columns;
- 5) load-deflection curves based on the cross-section analysis in the hypothesis of perfect bond between concrete and steel tubes allow acceptable prediction of experimental behavior.

## References

- Beedle, L.S. *et al.* (Editors), (1989), "Stability of metal structures", *A world view. 2<sup>nd</sup> ed. Structural Stability Research Council*, Bethlehem, Pa.
- Campione, G., Mindess, S., Scibilia, N. and Zingone, G. (1999), "Compressive behaviour of circular steel columns filled with fiber-reinforced concrete: experimental investigation and comparison with EC4 code", *Costruzioni Metalliche* **5**, 41-48.
- Campione, G., Mindess, S., Scibilia, N. and Zingone, G. (2000), "Strength of hollow circular steel sections filled with fibre-reinforced concrete", *Can. J. Civ. Eng.* **27**, 364-372.
- Campione, G., La Mendola, L., Scibilia N., Sanpaolesi L. and Zingone, G. (2001), "Behavior of fiber-reinforced concrete filled tubular columns in compression", *Material and Structures*, **35**, 332-337.
- CSA (1994), "Limit states design of steel structures. Standard CSA S16.1-94", Canadian Standards Association, Rexdale, Ont.
- Cosenza, E. and Pecce E.M. (2000), "Le colonne composte acciaio-calcestruzzo: analisi sperimentali, modelli di calcolo, indicazioni normative", *Costruzioni Metalliche*, **2**, 49-60 (only available in Italian).
- Cusson, D. and Paultre, P. (1995), "Stress-strain model for confined high-strength concrete", *J. Struct. Engng. ASCE*, **121** 3, 468-477.
- Eurocode 4 (1994), "Design of composite steel and concrete Structures", European Committee for Standardization (CEN), ENV 1994-1-1.
- Felicetti, R. and Gambarova, P.G. (1998), "Effects of high temperature on the residual compressive strength of high-strength siliceous concretes", *ACI Materials Journal*, **95** 4, 395-406.
- Han L., Zhao, X. and Tao, Z. (2001), "Tests and mechanics model for concrete-filled SHS stub columns, columns and beam-columns", *Steel & Composite Structures*, **1** 1, 51-74
- Issa, M.A. and Tobaa, H. (1994), "Strength and ductility enhancement in high-strength confined concrete", *Magazine of Concrete Research* **46**(168), 177-189.
- Johansson, M. and Kent, G. (2001), "Structural behavior of slender circular steel-concrete composite columns under various means of load application", *Steel & Composite Structures*, **1**(4), 393-410.
- Manual of Steel Construction, "Load and resistance factor design (LRFD) 1994", *2nd Ed., Am. Inst. of Steel Constr.* Chicago, Ill.

- Prion, H., G.L. and Boheme, J. (1993), "Beam-column behaviour of steel tubes filled with high strength concrete", *Can. J. Civ. Eng.*, **21**, 207-218.
- Shams, M. and Saadeghvaziri, M.A. (1997), "State of the art concrete-filled steel tubular columns", *ACI Struct. Journal*, **94**(5), 558-571.
- Sohal, I.S. and Chen, W.F. (1987), "Local buckling and sectional behavior of fabricated tubes", *J. Struct. Eng.*, ASCE **113**(4), 519-533.
- Sohal, I.S. and Chen W.F. (1988), "Local and post-buckling behavior of tubular beam-columns", *J. Struct. Eng.*, ASCE **114**(5), 1073-1089.
- Schneider, S.P. (1998), "Axially loaded concrete-filled steel tubes", *J. Struct. Eng.* ASCE, **124**(10), 1125-1138.
- Uy, B. (2000), "Strength of concrete filled steel box columns incorporating local buckling", *J. Struct. Eng.* ASCE, **126**(3), 341-352.
- Kodur, V.K.R. and Lie, T.T. (1995), "Fire resistance of hollow steel columns filled with steel fibre-reinforced concrete", *Fiber-reinforced Concrete. Modern Developments*, The University of British Columbia, Vancouver, Canada, Ed. N. Banthia, S. Mindess, 289-302.

## Notation

- $a$  : shear span in the four-point bending test
- $A_c$  : area of concrete core in the cross-section
- $A_s$  : area of steel cross-section
- $b$  : distance between the loads in four point bending test
- $D$  : external diameter of circular cross-section
- $E$  : elastic modulus of steel
- $E_c$  : modulus of elasticity of concrete in compression
- $E_{ct}$  : modulus of elasticity of concrete in tension
- $f_c$  : cylindrical compressive strength of concrete at 28 days
- $f_{ct}$  : tensile strength of plain concrete (or FRC)
- $f_r$  : post-peak strength in tension of FRC
- $f_y$  : yielding stress of steel
- $f_u$  : ultimate stress of steel
- $H$  : external length of the side in square cross-section
- $h$  : internal length of the side in square cross-section
- $L$  : length of the beam
- $L_c$  : length of the column
- $L_f$  : equivalent length of the fiber
- $M_u$  : bending moment at ultimate state
- $N_u$  : axial force at ultimate state
- $n$  : ratio between  $E_c$  and  $E$
- $n'$  : ratio between  $E_{ct}$  and  $E_c$
- $P$  : load in flexure test
- $P_v$  : load in compressive test
- $P_{max}$  : maximum compressive load
- $r$  : radius of circular cross-section in axis
- $t$  : thickness of the steel profile
- $x_c$  : neutral axis depth
- $\beta$  : angle that failure plane forms with the vertical direction
- $\phi$  : diameter of the fiber
- $\epsilon_u$  : ultimate strain of steel
- $\epsilon_y$  : yielding strain of steel
- $\sigma_s$  : axial stress in steel
- $\epsilon$  : longitudinal axial strain

- $\varepsilon_y$  : yielding strain of steel
- $\varepsilon_{ct}$  : strain of concrete in tension at peak load
- $\delta$  : deflection of the beam
- $\delta_v$  : axial shortening of the column
- $\theta$  : center angle in circular cross-section
- $\chi$  : flexural curvature
- $\chi_y$  : distance of the first section to yield
- $\chi_y$  : curvature at steel yielding
- $\chi_{\max}$  : ultimate curvature